Fractional Generalized Cauchy Prediction Model with 1/f Process for RUL of Rolling Bearing

Wei Cheng , Hongqing Zheng , Wanqing Song * , Piercarlo Cattani

Posted Date: 18 May 2026

doi: 10.20944/preprints202605.1129.v1

Keywords: 1/f process; Hurst exponent; fractal dimension; fractional; health indicator; bearing

 doi:10.20944/preprints202605.1129.v1

Article

Fractional Generalized Cauchy Prediction Model with 1/f Process for RUL of Rolling Bearing

Wei Cheng [1], Hongqing Zheng [1], Wanqing Song [1,*] and Piercarlo Cattani [2]

[1] School of Electronic and Electrical Engineering, Minnan University of Science and Technology, Quanzhou 362700, China

[2] Department of Computer, Control and Management Engineering, University of Rome La Sapienza, Via Ariosto 25, 00185 Roma, Italy

* Correspondence: zhqmnust@126.com

Abstract

Aiming at the non-stationary and slowly varying stochastic nature of bearing degradation from normal operation to failure, this paper proposes a fratcional Generalized Cauchy (fGC) prediction model with 1/f process and dual parameters: fractal dimension and Hurst exponent. First, 1/f process sequences exhibit long-range dependence and power-law characteristics. Next the fGC degradation model is established, and the Hurst exponent and fractal dimension are calculated using the R/S method and box-counting dimension method, respectively. Then a dimensionless jump descriptor is employed as a Health Indicator to detect incipient faults and estimate degradation parameters. The maximum likelihood algorithm method is applied to parameter estimation. Finally, a experiment verifies the satisfactory prediction performance through compared with CNN and LSTM predicting model.

Keywords: 1/f process; Hurst exponent; fractal dimension; fractional; health indicator; bearing

1. Introduction

Rolling bearings are widely used in various engineering fields and represent some of the most fundamental yet failure-prone components. Statistics show that nearly 30% of machine vibration faults are caused by bearing damage. Therefore, research on bearing remaining useful life (RUL) carries important theoretical and engineering significance.

Current artificial intelligence (AI) algorithms have been widely applied in RUL prediction research. In the field of RUL prediction, conventional machine learning methods, including regression analysis, support vector machines (SVM), and decision trees [1], are commonly adopted. Pugalenthi et al. [2,3] used a feed-forward ANN to predict the degradation trend of resistance, while also investigating the effects of noise and the number of hidden neurons. Kadir et al. [4,5] employed statistical parameters of the Weibull distribution as ANN inputs, thereby reducing noise interference. Reference [6] combined ANN with theory fatigue damage accumulation to achieve precise RUL prediction for cranes. Despite their effectiveness, these approaches are constrained by several drawbacks, including the tendency to fall into local optima, high expenses associated with model design and computation, and challenges in directly quantifying the uncertainty inherent in predictions. Long short-term memory (LSTM) networks are widely recognized as effective methods for RUL prediction. Reference [7] proposed a CNN comprising three convolutional layers and three fully connected layers, where were employed for feature extraction and the fully connected layers for forecasting sequential changes. Another strategy uses wavelet transform to extract detailed time-frequency information, followed by a multi-modal CNN for RUL [8]. In prior research [9,10], researchers successfully predicted the degradation tendency of rolling bearings by eliminating the Softmax classification layer from the CNN and incorporating three fully connected layers for model training. Nevertheless, deep learning models often struggle to directly capture temporal

 doi:10.20944/preprints202605.1129.v1

dependencies in degradation data. To overcome this limitation, the study reported in [11] combined multi-scale permutation entropy with LSTM: the multi-scale permutation entropy algorithm was utilized to detect sudden changes in equipment degradation, and the various degradation trends were then input into the LSTM model for prediction. Reference [12] established an LSTM prediction model for weak fault features in wind turbine rolling bearings using vibration and acoustic signals.

Artificial intelligence methods are purely data-driven and do not consider the physical degradation process. Such models typically require a large amount of case data for training.

Under actual engineering conditions, the bearing degradation process exhibits randomness and nonlinearity due to random fluctuations in operating conditions. The use of stochastic processes to characterize degradation is therefore more consistent with engineering reality. Reference [13] investigated RUL prediction based on the Gamma process, and [14] studied RUL prediction using a non-stationary Gamma process.

In addition, the Wiener process is another stochastic process widely used in degradation prediction. Reference [15] embedded physics-informed neural networks (PINN) into the Wiener process framework, using prior physical laws to constrain model training and improve generalization under small-sample conditions. This method is suitable for scenarios with incomplete degradation data and realizes a hybrid “mechanism + data” driven model. Reference [16] proposed a Wavelet Kernel Net-BiGRU-Wiener joint model, in which a deep network first constructs a health indicator(HI), which is then input into a Wiener process for reliability evaluation and uncertainty quantification. Reference [17] established a linear drift Wiener degradation model with a random drift coefficient. Reference [18] developed a bivariate prediction model based on a generalized nonlinear Wiener process and a shared frailty factor to handle complex systems with coupled multi-performance indicator degradation. The nonlinear drift term adopts a power-law function, and the shared factor captures individual heterogeneity.

Current stochastic prediction models assume that the increments of the degradation sequence process are independent, meaning they follow a Markov process. This independence assumption facilitates convenient modeling and computation. However, in practical engineering, most degradation processes are non-Markovian, with dependencies between increments, i.e., long-range dependence.

LRD models include the ON/OFF model [19,20]. In fields such as communication networks, neural signals, and financial time series, the combination of LRD and ON/OFF state-switching processes has been extensively studied as a core framework for modeling bursty, heavy-tailed, and persistently correlated systems. Although the term “LRD ON/OFF model” is not standard, it essentially refers to regenerative ON/OFF processes with heavy-tailed active and idle periods, which can naturally generate long-memory characteristics.

The ON/OFF model is a physically interpretable model with clear physical meaning. However, for complex practical scenarios, simulation and performance analysis are often challenging, and its underlying assumptions frequently deviate from engineering practice.

The FARIMA model [21,22] can characterize both long-range and short-range dependence. Furthermore, stronger LRD in the degradation process leads to better prediction performance, but computational efficiency is relatively low. Reference [23] took the degradation of a high-pressure compressor as the monitoring object and applied the FBM model to predict the RUL of turbofan engines. Reference [24] proposed an RUL estimation framework based on nonlinear diffusion FBM, modeling the degradation rate as a state-dependent function and introducing fractional Brownian motion to capture LRD. Reference [25] established an adaptive drift FBM model, which dynamically adjusts drift parameters through an online learning mechanism to handle sudden jumps.

In degradation modeling, FBM retains the randomness of Brownian motion while introducing LRD. However, in FBM, the Hurst exponent and fractal dimension have a fixed linear relationship, meaning degradation can only be described by a single parameter.

This paper proposes the GC process as an extension of the Cauchy process, which can characterize both short-range and LRD in nonlinear random series. The GC process overcomes the

 doi:10.20944/preprints202605.1129.v1

single-parameter limitation of FBM and includes two independent parameters—the Hurst exponent and fractal dimension—to describe LRD. A dual-parameter GC process is used to establish a degradation model for bearing RUL prediction, significantly improving prediction accuracy. A statistical method based on Monte Carlo theory is applied to obtain the probability density function (PDF) of RUL predictions.

The structure of this paper is organized as follows: Section 2 derives the LRD and power-law properties of 1/f process sequences; Section 3 derives the dual parameters of the autocorrelation function (ACF) of the Cauchy process, namely the Hurst exponent and fractal dimension; Section 4 constructs a degradation model based on the GC process; Section 5 presents the parameter estimation method for the proposed GC degradation model; Section 6 provides a case study of RUL prediction, including HI construction, incipient fault detection, error evaluation and discussion, as well as the solution methods for the Hurst exponent and fractal dimension; Section 7 concludes the paper.

2. LRD with 1/f Process

Let the ACF spectral density of a stochastic sequence $x(t)$ be $S_{xx}(\omega)$, then:

$$S_{xx}(\omega)=F\left[R_{xx}(\tau)\right]=\int_{-\infty}^{\infty}R_{xx}(\tau)e^{-i\omega\tau}d\tau, \tag{1}$$

when $\omega\to 0$, if existing:

$$S_{xx}(0)=F\left[R_{xx}(\tau)\right]=\int_{-\infty}^{\infty}R_{xx}(\tau)d\tau=\infty, \tag{2}$$

Then the ACF is non-integrable, exhibits power-law properties, and $x(t)$ is said to have LRD, indicating the value at any future time depends on the historical values of the sequence. Equation (2) can be rewritten as:

$$S_{xx}(\omega)=\frac{1}{f},\ f\to 0\ (\omega=2\pi f) \tag{3}$$

Any stochastic process $x(t)$ whose spectral density exhibits such LRD and power-law properties is referred to as a 1/f process, as shown in Figure 1.

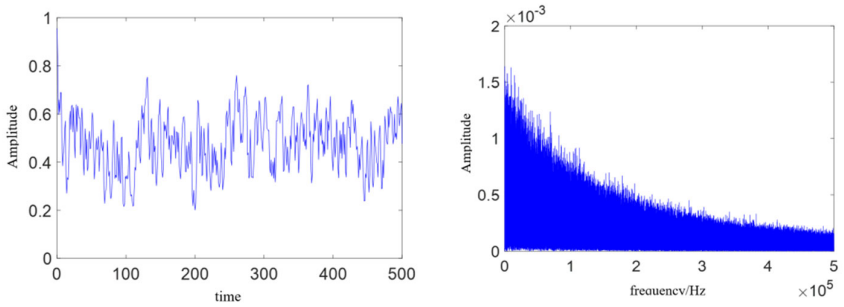

(a) $1/f$ process (b) Spectral density function

Figure 1. Simulation of $1/f$ process.

3. Dual Parameters of the Cauchy Process ACF: Hurst Exponent and Fractal Dimension

For a Cauchy sequence, its ACF [26] is:

$$C(\tau)=\left(1+|\tau|^2\right)^{-b/2},\ b>0 \tag{4}$$

τ is the time interval. When $\tau\to\infty$, $C(\tau)\sim\tau^{-b}$ exhibits power-law characteristics, and its integral:

 doi:10.20944/preprints202605.1129.v1

$$\int_0^\infty C_4(\tau)d\tau = \int_0^\infty \left(1+\tau^2\right)^{-b/2} d\tau = \begin{cases} \frac{1}{2}B\left(\frac{1}{2},\frac{b-2}{2}\right), & b>1 \\ \infty, & 0<b<1 \end{cases} \tag{5}$$

where $B(\cdot)$ denotes the beta function. Clearly, the $0<b<1$ exhibits LRD, while $b>1$ is short-range dependence . Using the Hurst exponent to describe this characteristics:

$$H = 1-\frac{b}{2} \tag{6}$$

then Equation (4):

$$C(\tau) = \left(1+|\tau|^2\right)^{H-1} \tag{7}$$

Figure 2 shows the ACF of the Cauchy process. When $0.5<H<1$, it is a LRD process and 1/f process; when $H<0.5$, it is a short-range dependence process.

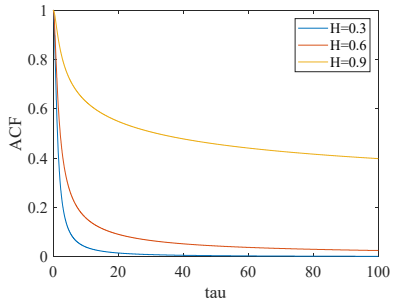

Figure 2. The ACF of Cauchy process.

When $\tau \to 0$, we have:

$$C(0)-C(\tau) \sim |\tau|^a \tag{8}$$

The fractal dimension of $C(\tau)$ is $D=2-a/2$. Replacing all parameters with the Hurst exponent H and fractal dimension D, $C(\tau)$ becomes:

$$C(\tau) = \left(1+|\tau|^{4-2D}\right)^{\frac{1-H}{2-D}},\ 1<D<2,\ 0.5<H<1 \tag{9}$$

The ACF with dual parameters can describe the characteristics between D and H. Figure 3 also shows a larger Hurst exponent results in stronger power-law behavior, i.e., stronger LRD; while a higher D leads to lower correlation.

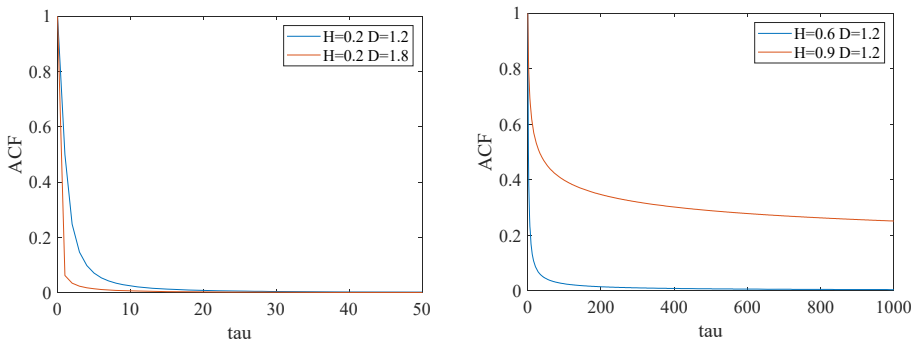

Figure 3. The ACF simulation of GC process.

 doi:10.20944/preprints202605.1129.v1

4. fGC Degradation Model

In terms of Itô process definition [26], the SDE for the GC process is defined below:

$$dX(t) = f(t)dt + g(t)dGC_{D,H}(t) \tag{10}$$

Referring to[27], certain simplifications is applied in the modeling process: let $g(t)$ be a constant, Equation (10) becomes:

$$dX(t) = \mu(t;\boldsymbol{\theta})dt + \sigma_{D,H}dGC_{D,H}(t) \tag{11}$$

where $\mu(t;\theta)$ is the nonlinear drift term, which combines a constant and a function describing the trend form, i.e. $\mu(t;\boldsymbol{\theta}) = \alpha\varphi(t)$,where $\varphi(t)$ express the overall trend in the degradation process, and α is a constant. $\sigma_{D,H}$ is the diffusion coefficient, representing randomness during the degradation process. Equation (11) is discretized and convert it into difference form, the the expression is given by:

$$\Delta X(t) = \alpha[\varphi(t+\Delta t) - \varphi(t)] + \sigma_{D,H}\Delta GC_{D,H}(t) \tag{12}$$

fGC predicting model is obtained, as shown in Equation (13):

$$x(t) = x(0) + \int_0^t \alpha\varphi(t)dt + \sigma_{D,H}\Delta GC_{D,H}(t) \tag{13}$$

Once the parameters D and H are determined, the increments $\Delta GC_{D,H}(t)$ of the GC process is as follows:

1) Based on the known sequence $X(t)$, generate a numerical sequence of the GC process;

2) Determine the time interval τ , $\Delta GC_{D,H}(t)$ difference is

$$\Delta GC_{D,H}(t) = GC_{D,H}(t+\tau) - GC_{D,H}(t) \tag{14}$$

3) Repeat step 2, performing multiple differences on the generated time series to constitutea set of increments $\Delta GC_{D,H}(t)$;

4) The increments at interval τ obey a Gaussian distribution $GC_{D,H}(\tau) \sim N(0,\sigma_\tau)$, solution variance σ_τ;

5) Generate increments from the determined Gaussian distribution.

Figure 4 shows that the increments follow an approximate Gaussian distribution based on extensive numerical simulations; Figure 5 illustrates that the approximation improves as the number of simulations increases.

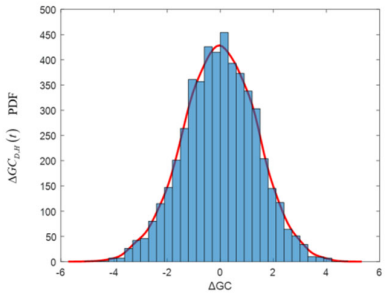

Figure 4. probability distribution of GC increment.

 doi:10.20944/preprints202605.1129.v1

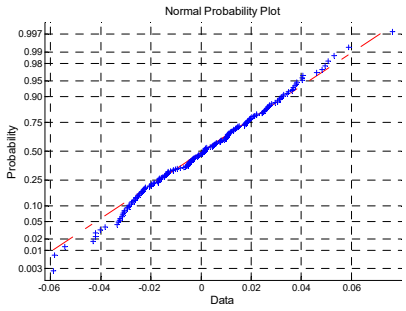

Figure 5. Normality test of GC increment.

5. Parameter Estimation for the fGC Degradation Model

The k historical data from t_0 to t_k are written in vector form as $\mathbf{X}=[X_0,X_1,...,X_k]^{\mathrm{T}}$, and the increment vector of this vector $\mathbf{X}$ is $\mathbf{Y}=[X_1-X_0,X_2-X_1,.....,X_k-X_{k-1}]^{\mathrm{T}}$. According to the Gaussian process property of the GC process, $\mathbf{Y}$ the vector follows a multivariate normal distribution with $\mathbf{Y}\sim\mathcal{N}(\alpha\boldsymbol{\varphi},\sigma^2\mathbf{Q})$. Here, $\alpha\boldsymbol{\varphi}$ is the mean vector,

$$\boldsymbol{\varphi}=\left[\gamma(t_1),\gamma(t_2),...,\gamma(t_k)\right]^{\mathrm{T}}, \tag{15}$$

Each element in the vector $\boldsymbol{\varphi}$ is $\gamma(t_i)=\varphi(t_i)-\varphi(t_{i-1})$. $\sigma^2\mathbf{Q}$ is a covariance matrix, where each element in $\mathbf{Q}$ has:

$$Q_{ij}=\left(1+\left(|i-j|\tau\right)^{4-2D}\right)^{\frac{1-H}{2-D}}. \tag{16}$$

where Q_{ij} indicates the position of each element in the k-dimensional matrix. Thus, the $\mathbf{Y}$ vector's PDF can be expressed as:

$$f(\mathbf{Y})=\left(2\pi\sigma^2\right)^{-k/2}|\mathbf{Q}|^{-1/2}\exp\left\{-\frac{1}{2\sigma^2}\times(\mathbf{Y}-a\boldsymbol{\varphi})^{\mathrm{T}}\mathbf{Q}^{-1}(\mathbf{Y}-a\boldsymbol{\varphi})\right\} \tag{17}$$

The log-likelihood function of the Equation(18) is:

$$l(\boldsymbol{\theta}|\mathbf{X})=-\frac{k}{2}\ln(2\pi)-k\ln\sigma-\frac{1}{2}\ln|\mathbf{Q}|-\frac{1}{2\sigma^2}(\mathbf{Y}-\alpha\boldsymbol{\varphi})^{\mathrm{T}}\mathbf{Q}^{-1}(\mathbf{Y}-\alpha\boldsymbol{\varphi}) \tag{18}$$

Next, the partial derivatives of the formula (19) about α and σ^2, and let the partial derivatives to zero, i.e., the following form:

$$\begin{aligned}\frac{\partial\ell}{\partial\alpha}&=\frac{\partial\left(-\frac{k}{2}\ln(2\pi\sigma^2)-\frac{1}{2}\ln|\mathbf{Q}|-\frac{1}{2\sigma^2}(\mathbf{Y}-\alpha\boldsymbol{\varphi})^{\mathrm{T}}\mathbf{Q}^{-1}(\mathbf{Y}-\alpha\boldsymbol{\varphi})\right)}{\partial\alpha}\\&=\frac{\partial\left(-\frac{1}{2\sigma^2}(\mathbf{Y}-\alpha\boldsymbol{\varphi})^{\mathrm{T}}\mathbf{Q}^{-1}(\mathbf{Y}-\alpha\boldsymbol{\varphi})\right)}{\partial\alpha}\\&=\frac{\partial\left(-\frac{1}{2\sigma^2}\left(\mathbf{Y}^{\mathrm{T}}\mathbf{Q}^{-1}\mathbf{Y}-\alpha\boldsymbol{\varphi}^{\mathrm{T}}\mathbf{Q}^{-1}\mathbf{Y}-\mathbf{Y}^{\mathrm{T}}\mathbf{Q}^{-1}\alpha\boldsymbol{\varphi}+\alpha^2\boldsymbol{\varphi}^{\mathrm{T}}\mathbf{Q}^{-1}\boldsymbol{\varphi}\right)\right)}{\partial\alpha}\\&=-\frac{\left(-\boldsymbol{\varphi}^{\mathrm{T}}\mathbf{Q}^{-1}\mathbf{Y}-\mathbf{Y}^{\mathrm{T}}\mathbf{Q}^{-1}\boldsymbol{\varphi}+2\alpha\boldsymbol{\varphi}^{\mathrm{T}}\mathbf{Q}^{-1}\boldsymbol{\varphi}\right)}{2\sigma^2}=0\end{aligned} \tag{19}$$

The maximum likelihood estimate for α is:

$$\hat{\alpha}=\frac{\boldsymbol{\varphi}^{\mathrm{T}}\mathbf{Q}^{-1}\mathbf{Y}}{\boldsymbol{\varphi}^{\mathrm{T}}\mathbf{Q}^{-1}\boldsymbol{\varphi}} \tag{20}$$

 doi:10.20944/preprints202605.1129.v1

$$\frac{\partial \ln g(\mathbf{Y})}{\partial \sigma^2} = \frac{\partial\left(-\frac{k}{2}\ln(2\pi\sigma^2)-\frac{1}{2}\ln|\mathbf{Q}|-\frac{1}{2\sigma^2}(\mathbf{Y}-\alpha\boldsymbol{\varphi})^{\mathrm{T}}\mathbf{Q}^{-1}(\mathbf{Y}-\alpha\boldsymbol{\varphi})\right)}{\partial\sigma^2} = -\frac{k}{2\sigma^2}+\frac{(\mathbf{Y}-\alpha\boldsymbol{\varphi})^{\mathrm{T}}\mathbf{Q}^{-1}(\mathbf{Y}-\alpha\boldsymbol{\varphi})}{2(\sigma^2)^2}=0 \tag{21}$$

$$\sigma^2 = \frac{(\mathbf{Y}-\alpha\boldsymbol{\varphi})^{\mathrm{T}}\mathbf{Q}^{-1}(\mathbf{Y}-\alpha\boldsymbol{\varphi})}{k}. \tag{22}$$

the maximum likelihood estimate for σ^2 is:

$$\hat{\sigma}^2 = \frac{1}{k}\frac{(\mathbf{Y}^{\mathrm{T}}\mathbf{Q}^{-1}\mathbf{Y})(\boldsymbol{\varphi}^{\mathrm{T}}\mathbf{Q}^{-1}\boldsymbol{\varphi})-(\boldsymbol{\varphi}^{\mathrm{T}}\mathbf{Q}^{-1}\mathbf{Y})^2}{\boldsymbol{\varphi}^{\mathrm{T}}\mathbf{Q}^{-1}\boldsymbol{\varphi}} \tag{23}$$

6. RUL Prediction for Bearing Outer Race

6.1. Testing Platform

To validate the effectiveness of the proposed method. This experiment uses the LDK UER204 rolling bearing to conduct accelerated failure tests on rolling elements. The experimental platform constructed is demonstrated in Figure 6, the bearing test setup is composed of an alternating current (AC) motor, a motor speed regulator, a supporting shaft, two supporting bearings, a hydraulic loading mechanism, and additional auxiliary parts. A radial load is produced by the hydraulic loading mechanism and exerted on the test bearing's housing. The AC motor's speed regulator is responsible for setting and sustaining the rotational speed. Table 1 presents the specifications of the tested bearing.

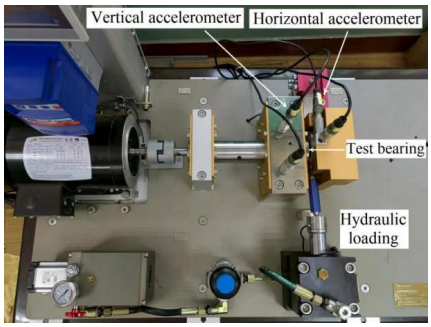

Figure 6. Bearing experimental platform.

Table 1. Design tested parameter.

parameter	value	parameter	value
Outer race diameter	39.80mm	Inner race diameter	29.30mm
Bearing pitch diameter	34.55mm	Roller diameter	7.92mm
Number of rollers	8	Contact angle	0°
Static load rating	6.65kN	Dynamic load rating	12.82kN

Two acceleration sensors PCB 352C33 are erected on the test bearing in the horizontal and vertical directions, respectively. The sampling frequency is 25.6 kHz, with 32768 data points collected per acquisition time and a collection interval of 1 minute. The bearing rotational speed is set to 2100 rpm (35 Hz), and a radial load of 12kN is applied via the hydraulic system. The test is terminated when the maximum amplitude exceeds 10 times the average amplitude during normal operation, the test stops, as shown in Figure 7.

 doi:10.20944/preprints202605.1129.v1

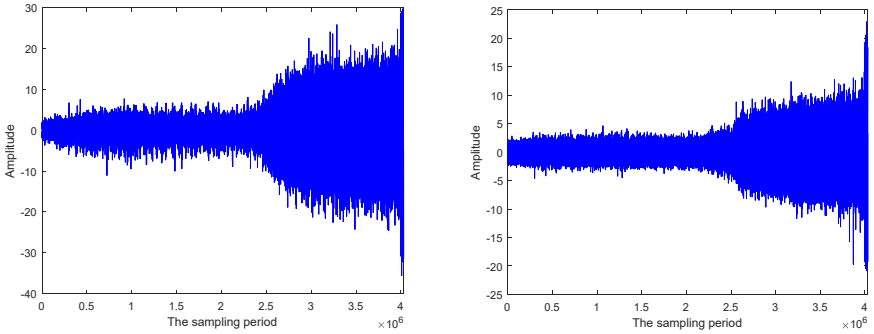

(a) Horizontal vibration signal (b) Vertical vibration signal

Figure 7. Acquisition signal for outer race fault.

Figure 7 exhibits that the bearing vibration signal collected by the horizontal sensor is more pronounced. Therefore, the vibration signal of the horizontal direction is used for prediction.

6.2. HI and Incipient Fault Initiation Detection

The transition from normal operation to severe failure is a slow evolutionary process. Once an incipient fault develops in the bearing, the component enters the progressive degradation stage. Early detection of such incipient faults is critically important, but these weak fault features are often submerged in strong noise. A core challenge is selecting proper health indicators to identify incipient faults from the strong noise and degradation parameter is the core of achieving accurate RUL prediction.

Bearing HI can be divided into two categories: time-domain and frequency-domain indicator. Frequency-domain include waveform indicator, peak indicator, impulse indicator, margin indicator, kurtosis indicator, and skewness indicator. These parameters are related to bearing vibration energy, and show different sensitivities to different fault types and degradation degrees of bearings. Based on time-domain waveform statistical analysis, several new energy-insensitive dimensionless amplitude-domain parameters are constructed: repeatability descriptor, similarity descriptor, and jump descriptor. These parameters can quantitatively analyze the fault-related waveform shape information, and can well reflect the evolution trend of bearing faults under varying load conditions. The experiment in this paper shows that the jump descriptor has the highest sensitivity to bearing degradation, and its calculation algorithm is as follows:

(1) the sampling raw data sequences is segmented into n waveform data with m long sub-sequence

$$\{x_{11},x_{12},\cdots,x_{1m};\cdots;x_{n1},x_{n2},\cdots,x_{nm}\} \tag{24}$$

(2) Extract each sub-sequence as $x_{11},x_{12},\cdots,x_{1m}$ the minimum values $x_{\min}=x_{1p},1<p<m$ from the segmented data and calculate their mean value

$$\bar{x}=\frac{1}{n}\sum_{i=1}^{n}x_{ip} \tag{25}$$

(3) Calculate the variance of the above minimum values

$$D_x=\frac{1}{n}\sum_{i=1}^{n}(x_{ip}-\bar{x})^2 \tag{26}$$

The jump descriptor is defined $J_f=D_x$, it is a non-dimensional parameter.

 doi:10.20944/preprints202605.1129.v1

The HI curve based on the jump descriptor is shown in Figure 8. Obviously, the degradation process is effectively extracted, and an incipient fault occurs at approximately the 310th point in this experiment.

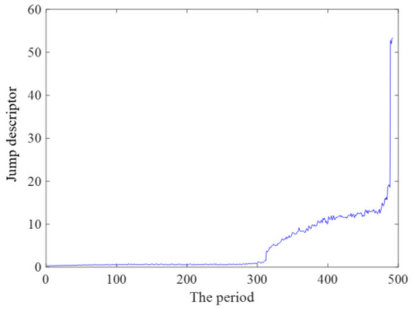

Figure 8. Outer race fault degradation process after feature extraction.

6.3. Parameter Estimation for H, D and fGC Model

The R/S method [29] and the box-counting dimension [30] are used to calculate the values of the Hurst exponent and fractal dimension, respectively, and the maximum likelihood estimation is applied to obtain the model parameters, see Figure 9, Figure 10 and Table 2.

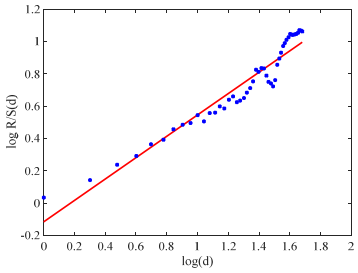

Figure 9. Least squares fitting of Hurst using R.S

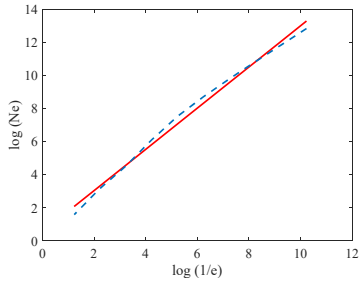

Figure 10. Least squares fitting of fractal dimension.

Table 2. Parameter value estimated for the GC prediction model.

	H	D	μ	σ
GC	0.8033	1.2117	0.0254	0.04638

6.4. Prediction Result and Evaluation Discussion

Based on the bearing degradation process analysis, we compared and analyzed CNN, LSTM, and GC models, respectively. The prediction results of the GC degradation model and LSTM, CNN are shown in Figure 11. All predicted points fall within the reliable region, and the prediction accuracy meets the requirements. See Figure 12.

 doi:10.20944/preprints202605.1129.v1

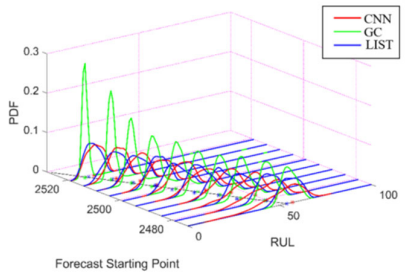

Figure 11. PDF of different model RUL prediction .

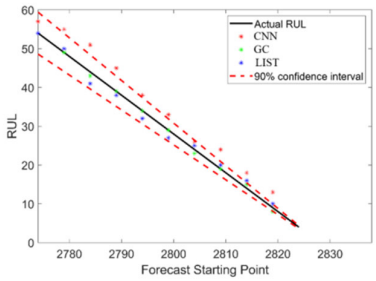

Figure 12. prediction result and confidence region.

Below four HI are applied to evaluate the prediction accuracy of the three models:

（1） Health Index (HD)

$$HD = 1 - \frac{\sum_{i=1}^{N}(R_i - Y_i)}{\sum_{i=1}^{N}(R_i - Mean)}, \tag{27}$$

where HI represents the health status of the prediction model, which is used to measure the performance of the prediction model. The closer the Health Index is to 1, the better the performance of the prediction model.

(2) Root Mean Square Error (RMSE)

A smaller value indicates better model performance.

$$RMSE = \sqrt{\frac{1}{n}\sum_{i=1}^{n}\left(Y_i - \hat{Y}_i\right)^2} \tag{28}$$

where Y_i is the true value, and $\hat{Y}_i$ is the predicted value.

(3) Mean Absolute Error (MAE)

A smaller value indicates better model performance.

$$MRE = \frac{1}{n}\sum_{i=1}^{n}\left|Y_i - \hat{Y}_i\right| \tag{29}$$

This indicator measures the prediction ability of the model, and the closer its value is to 1, the better the performance.

(4) Coefficient of Determination (R^2)

This indicator measures the prediction ability of the model, and the closer its value is to 1, the better the performance.

$$R^2 = 1 - \frac{\sum_{i=1}^{n}\left(Y_i - \hat{Y}_i\right)^2}{\sum_{i=1}^{n}\left(Y_i - \bar{Y}\right)^2} \tag{30}$$

where $\bar{Y}$ is the mean of the practice values.

 doi:10.20944/preprints202605.1129.v1

Table 3. prediction accuracy of three types prediction models.

	R^2	RMSE	MAE	HD
CNN	0.2580	3.5123	3.6800	0.8817
LSTM	0.6857	1.4273	1.3962	0.9023
GC	**0.8743**	**0.6241**	**0.4113**	**0.9845**

Table 3 presents the error evaluation results of the three models. The MAE and RMSE of the RUL predicted by the GC model are lower than the CNN and LSTM, while the HD and SOR of the GC model are higher than those of the other two models. As shown in Figure 12 and Table 3, the GC model is more suitable for bearing RUL prediction.

7. Conclusions

This paper proposes using the fractional GC prediction model with LRD and 1/f process for rolling bearings RUL prediction. Compared with other relevant models, it has the following advantages:

(1) LRD is consistent with the fact that the bearing degradation process is a slow, non-stationary stochastic process. The model determined by the dual parameters of fractal dimension and Hurst exponent is more suitable for practical engineering problems.

(2) Using the jump descriptor as a health indicator enables extraction of health indicator parameters from strong noise. As a predictive parameter for degradation, it can also detect the occurrence time of weak faults at an early stage.

(3) Experiments on the proposed test platform verify that the prediction accuracy of this paper model is higher than that of LSTM and CNN models.

(4) The limitations of the work: the data used are all obtained under stable laboratory operating conditions, which means the working conditions (rotational speed and load) for each dataset are fixed. In the actual operation of bearings, however, due to the inevitable random variations in operating environment and load, the rotational speed and torque of bearings also fluctuate randomly. Future research will focus on predicting degradation trends under time-varying operating conditions.

Author Contributions: Conceptualization, Wei C., Wanqing S.; methodology, Wei C., Wanqing S.; software, Wei C., Hongqing Z. and Piercarlo Cattani; formal analysis, Piercarlo Cattani; investigation, Hongqing Z.; resources,Wanqing S.; data curation,Wanqing S.; writing—original draft preparation, Wei C.; writing—review and editing, Piercarlo Cattani; supervision, Hongqing Z.; project administration, Hongqing Z.; All authors have read and agreed to the published version of the manuscript.

Funding: This research was funded by the Technology Innovation Project of Minnan University of Science and Technology, grant number 24XTD158, and the special fund for Science and Technology Innovation Teams of Shanxi Province (202304051001013)

Data Availability Statement: Where no new data were created, or where data is unavailable due to privacy or ethical restrictions

Conflicts of Interest: The authors declare no conflicts of interest. The funders had no role in the design of the study; in the collection, analyses, or interpretation of data; in the writing of the manuscript; or in the decision to publish the results.

References

1. PS Kumar, SK Laha, LA Kumaraswamidhas, Assessment of rolling element bearing degradation based on Dynamic Time Warping, Applied Acoustics, 2023, 199:108568
2. Pugalenthi K, Park H, Raghavan N. Prognosis of power MOSFET resistance degradation trend using artificial neural network approach, Microelectronics Reliability, 2019, 100-101:113467.

 doi:10.20944/preprints202605.1129.v1

3. Zhao W, Tao T, Zio E, et al. A Novel Hybrid Method of Parameters Tuning in Support Vector Regression for Reliability Prediction: Particle Swarm Optimization Combined With Analytical Selection, IEEE Transactions on Reliability, 2016, 65(3): 1393-1405.
4. Mahamad A K, Saon S, Hiyama T. Predicting remaining useful life of rotating machinery based artificial neural network, Computers & Mathematics with Applications, 2010, 60(4):1078-1087.
5. T Lin, H Wang, X Guo, P Wang, L Song, A novel prediction network for remaining useful life of rotating machinery, The International Journal of Advanced Manufacturing Technology, 2023, 124(11-12):1-10
6. Zhenwen Liu，Xuan Kong，Lu Deng, Prediction and Uncertainty Quantification of the Fatigue Life of Corroded Cable Steel Wires Using a Bayesian Physics-Informed Neural Network, Journal of Bridge Engineering, 2025, 30(5):04025018
7. Harbola S, Coors V. One dimensional convolutional neural network architectures for wind prediction, Energy Conversion and Management, 2019, 195:70-75.
8. Zhu J, Chen N, Peng W. Estimation of Bearing Remaining Useful Life Based on Multiscale Convolutional Neural Network, IEEE Transactions on Industrial Electronics, 2019, 66(4):3208-3216.
9. Thanh Q. Nguyen,Tu B. Vu, Niusha Shafiabady, Loss factor analysis in real-time structural health monitoring using a convolutional neural network, Archive of Applied Mechanics, 2024, 95:15
10. S Y Kim, M Mukhiddinov, Data Anomaly Detection for Structural Health Monitoring Based on a Convolutional Neural Network, Sensors, 2023, 23(20):8525
11. Chen, Guihui，Wei, Yuli，Peng, Jiao, Spatio-temporal graph neural network based on time series periodic feature fusion for traffic flow prediction , The Journal of Supercomputing, 2025, 81(1):129
12. Wang, Hongju，Zhang, Xi，Ren, Mingming, Remaining Useful Life Prediction of Rolling Bearings Based on Multi-scale Permutation Entropy and ISSA-LSTM, Entropy, 2023, 25(11):1477
13. Daniel Kuzio, Radosław Zimroz, Agnieszka Wyłomańska, A modified gamma process for RUL prediction based on data with time-varying heavy-tailed distribution, Information Sciences, 2025, 690(2):121603,
14. Naipeng Li, Mingyang Wang, Yaguo Lei, Bin Yang, Xiang Li, Xiaosheng Si, Remaining useful life prediction of lithium-ion battery with nonparametric degradation modeling and incomplete data, Reliability Engineering & System Safety, 2025, 256(4):110721.
15. Zhongze He, Shaoping Wang, Jian Shi, Di Liu, Xiaochuan Duan, Yaoxing Shang, Physics-informed neural network supported Wiener process for degradation modeling and reliability prediction, reliability engineering & system safety, 2025, 258(6):110906
16. Xiaofei Wang, BingXing Wang, PeiHua Jiang, Yili Hong, Accurate reliability inference based on Wiener process with random effects for degradation data, Reliability Engineering & System Safety, 2020, 193(1)：106631
17. Qingqing Zhai, Zhi-Sheng Ye, RUL Prediction of Deteriorating Products Using an Adaptive Wiener Process Model, IEEE Transactions on Industrial Informatics, 2017, 13(6):2911-2921
18. Lu Li, Zhihua Wang, Qiong Wu, Zelong Mao, Chengrui Liu, bivariate degradation modeling and reliability analysis based on generalized nonlinear wiener processes and a shared frailty factor, quality and reliability engineering international, 2024,
19. David Heath, Sidney Resnick, Gennady Samorodnitsky, Heavy Tails and Long Range Dependence in On/Off Processes and Associated Fluid Models, Mathematics of Operations Research，1998，23(1):145-165
20. Remigijus Leipus, Donatas Surgailis, On Long-Range Dependence in Regenerative Processes Based on a General ON/OFF Scheme, Journal of Applied Probability, 2006, 44(2):421-440
21. Jan Beran, Yuanhua Feng and Sucharita Ghosh, Modeling Long-Range Dependence in Financial Time Series Using FARIMA Models, Physica A: Statistical Mechanics and its Applications, 2015, 56(4):431-451
22. M. Grossglauser, J.-C. Bolot,FARIMA Modeling of Network Traffic with Long-Range Dependence, IEEE Transactions on Network Science and Engineering, 2024, 7(5):629-640
23. Xi X, Chen M, Zhou D., Remaining Useful Life Prediction for Degradation Processes With Memory Effects, IEEE Transactions on Reliability, 2017, 66(3): 751-760.

 doi:10.20944/preprints202605.1129.v1

24. Zhang X-W, Si X-S, Hu C-H, et al.,Remaining useful life estimation based on a nonlinear diffusion degradation process with fractional Brownian motion, Mechanical Systems and Signal Processing, 2023, 191:110165
25. Ali Asgari, Wujun Si, Wei Wei, et al., A degradation model for time-varying degradation processes based on fractional Brownian motion with adaptive drift, Reliability Engineering & System Safety, 2024, 248:110146
26. Chilès J-P, Delfiner P. Geostatistics: Modeling Spatial Uncertainty, 2nd Edition, Wiley, 2012.
27. Leonardo S. Lima,Nonlinear Stochastic Equation within an Itô Prescription for Modelling of Financial Market, entropy, 2019,21(5):530
28. Wang B, Lei Y, Li N. A Hybrid Prognostics Approach for Estimating Remaining Useful Life of Rolling Element Bearings, IEEE Transactions on Reliability, 2018: 1-12.
29. MS Li,XH Yang,BY Sun,Future trend analysis of precipitation in the Haihe River basin based on a method combining wavelet and rescaled range analyses,Thermal Science, 2018, 1571-1579
30. T. Ai, R. Zhang, H.W. Zhou,J.L. Pei,Box-counting methods to directly estimate the fractal dimension of a rock surface,applied surface science, 2014, 314(30):610-621